Annals of Botany **107**: 729–745, 2011
doi:10.1093/aob/mcq173, available online at www.aob.oxfordjournals.org

ANNALS OF BOTANY
Founded 1887

PART OF A SPECIAL ISSUE ON GROWTH AND ARCHITECTURAL MODELLING

Comparison of three approaches to model grapevine organogenesis in conditions of fluctuating temperature, solar radiation and soil water content

B. Pallas[1,2], C. Loi[2], A. Christophe[3], P. H. Cournède[2] and J. Lecoeur[1,*]

[1]*Montpellier SupAgro, Département Sciences du Végétal, 2, place Viala, F-34060 Montpellier, France,* [2]*Ecole Centrale de Paris – Laboratoire MAS, Grande voie des vignes, F-92 295 Châtenay-Malabry, France and* [3]*INRA Montpellier, UMR 759 LEPSE, 2 place Viala, F-34060 Montpellier, France*
** For correspondence. E-mail jeremie.lecoeur@supagro.inra.fr*

Received: 4 February 2010 Returned for revision: 4 May 2010 Accepted: 8 July 2010 Published electronically: 18 September 2010

• *Background and Aims* There is increasing interest in the development of plant growth models representing the complex system of interactions between the different determinants of plant development. These approaches are particularly relevant for grapevine organogenesis, which is a highly plastic process dependent on temperature, solar radiation, soil water deficit and trophic competition.
• *Methods* The extent to which three plant growth models were able to deal with the observed plasticity of axis organogenesis was assessed. In the first model, axis organogenesis was dependent solely on temperature, through thermal time. In the second model, axis organogenesis was modelled through functional relationships linking meristem activity and trophic competition. In the last model, the rate of phytomer appearence on each axis was modelled as a function of both the trophic status of the plant and the direct effect of soil water content on potential meristem activity.
• *Key Results* The model including relationships between trophic competition and meristem behaviour involved a decrease in the root mean squared error (RMSE) for the simulations of organogenesis by a factor nine compared with the thermal time-based model. Compared with the model in which axis organogenesis was driven only by trophic competition, the implementation of relationships between water deficit and meristem behaviour improved organogenesis simulation results, resulting in a three times divided RMSE. The resulting model can be seen as a first attempt to build a comprehensive complete plant growth model simulating the development of the whole plant in fluctuating conditions of temperature, solar radiation and soil water content.
• *Conclusions* We propose a new hypothesis concerning the effects of the different determinants of axis organogenesis. The rate of phytomer appearance according to thermal time was strongly affected by the plant trophic status and soil water deficit. Futhermore, the decrease in meristem activity when soil water is depleted does not result from source/sink imbalances.

Key words: Thermal time, trophic competition, axis organogenesis, soil water deficit, plant growth models, phenotypic plasticity, grapevine, *Vitis vinifera*.

INTRODUCTION

As in other species with an indeterminate pattern of development [e.g. white clover (Belaygue *et al.*, 1996) or pea (Turc and Lecoeur, 1997)] axis organogenesis in grapevine displays strong phenotypic plasticity in fluctuating environments (Lebon *et al.*, 2004). Axis organogenesis is highly variable, and the number of developing leaves may be ten times higher in optimal conditions than in poor environments (Pallas *et al.*, 2010). Moreover, a number of routine practices in viticulture, such as pruning (Rives, 2000) and irrigation (Stevens *et al.*, 2008), were empirically developed to optimize yield and cluster quality by modifying axis organogenesis.

Axis organogenesis in grapevine has been shown to be driven by temperature (Schultz, 1992), photosynthetically active radiation (Pallas *et al.*, 2010) and soil water content (Lebon *et al.*, 2006). Grapevine organogenesis also depends on the source–sink relationships (Wardlaw, 1990) between organs (Pallas *et al.*, 2008) and the anatomical structure of the shoot (Jaquinet and Simon, 1971). The grapevine shoot is a modular branching system with one primary and many secondary axes organized into structures consisting of three successive phytomers (P0–P1–P2). P0 phytomers bear no tendril or clusters. Phytomers bearing tendrils or clusters are classified as P1 or P2 phytomers. This modular structure also modifies the development of the secondary axis. The secondary axes born by the P0 phytomer (hereafter referred to as P0 secondary axes) develop more strongly than those arising from P1–2 phytomers (hereafter referred to as P1–P2 secondary axes) (Louarn *et al.*, 2007). Furthermore, the P1 and P2 secondary axes do not display differences in organogenesis or morphogenesis processes (Lebon *et al.*, 2004). The impact of the various microclimatic variables affecting axis organogenesis has been estimated or evaluated by considering each factor independently. Nevertheless the interactions between the different processes driving plant development, such as photosynthetic activity, rate of axis development and trophic competition, have yet to be quantified. Many authors suggested that the best way to analyse this system would be to model the complex system of interactions between plant development,

plant functioning and microclimate conditions (Dingkuhn *et al.*, 2005).

In this study, the aim was to develop three plant growth models to determine (*a*) whether it was necessary to include trophic competition between organs in models of axis organogenesis and (*b*) whether this consideration of trophic competition is sufficient for the modelling of axis organogenesis in fluctuating environmental conditions, including soil water deficit. In this study, the various environmental conditions were related to the level of incident radiation, temperature and soil water content. Axis organogenesis variation and grapevine whole-plant development have never before been modelled in terms of the combination of these three environmental variables in a whole-plant growth model. These variables have an impact on the trophic status of the plant which in turn affects axis organogenesis (Pallas *et al.*, 2009). Indeed, photosynthetically active radiation (Monteith, 1977), soil water content (Hsiao, 1973) and temperature (Johnson and Thronley, 1985) modify the amount of assimilate produced, through direct effects on the photosynthetic activity of leaves and plant leaf area dynamics.

It has been suggested that there is no need to include carbon balance in models of plant development in the absence of soil water deficit. In that case, axis organogenesis is considered to be driven only by temperature, through thermal time (Chenu *et al.*, 2008). However, a number of studies coupling experimental analyses of plant organogenesis with modelling approaches to quantify trophic competition [EcoMeristem on rice (Luquet *et al.*, 2006) or GreenLab model on grapevine (Pallas *et al.*, 2009)] have indicated that secondary axis organogenesis is mainly driven by trophic competition. Conversely, for grapevine, primary axis organogenesis appeared to be only driven by temperature (Lebon *et al.*, 2004). Two models were therefore constructed, one based on the assumption that axis organogenesis is driven purely by thermal time and the other based on the control of meristem activity by trophic competition. The ability of these two models to simulate axis organogenesis in conditions of fluctuating solar radiation and temperature was assessed. Six experiments were carried out by varying the level of photosynthetic active radiation to test the ability of these two models to simulate axis organogenesis. To build the whole-plant model in which axis organogenesis was considered to depend on trophic competition, several formalisms previously proposed in the GreenLab approach (Yan *et al.*, 2004) were used. This model also includes several relationships between trophic competition and axis organogenesis which has been formalized before (Mathieu *et al.*, 2009).

Water deficit has been shown to have two main effects on plant physiology (Hsiao, 1973). Soil water deficit reduces the photosynthetic activity of the leaves (Schultz, 2003) and induces non-trophic processes (mechanistic or hormonal) that tend to limit whole-plant development (Tardieu *et al.*, 1999). These experimental results raise two key hypotheses for use in modelling approaches: (1) the variation in axis organogenesis with soil water content may result purely from the assimilate deficiency caused by the decrease in photosynthetic activity (Mathieu *et al.*, 2009); (2) plant organogenesis variation in conditions of fluctuating soil water content may be related to non-trophic determinants, such as hormonal signals (Sobeih *et al.*, 2004). The ability of the model including the effects of trophic competition at the plant scale to deal with the observed plasticity of plant development in conditions of water deficit was assessed. A plant growth model including the effects of both trophic competition and non-trophic determinants on axis organogenesis was also constructed and tested. The ability of these two models to deal with organogenesis plasticity was assessed by comparing simulations and observed data collected on plants subjected to different levels of water deficit. This approach made it possible to evaluate the part carbon limitation plays on axis organogenesis in conditions of water deficit.

MATERIALS AND METHODS

'Thermal time-based' model

Underlying concepts. The model is based on the assumption that axis organogenesis is driven by temperature alone (Schultz, 1992). The organogenesis processes on each axis are modelled assuming a constant rate of phytomer appearance and a given duration of development.

Thermal time calculation. Thermal time (T_d) is calculated by the daily integration of air temperatures after the subtraction of a base temperature of 10 °C (Lebon *et al.*, 2004) and it is expressed in degree-days (°Cd) from budburst.

Primary axis organogenesis. The change in the number of phytomers on the primary axis $N_I(T_d)$ is expressed as a linear function of thermal time (Schultz, 1992; Lebon *et al.*, 2004).

$$N_I(T_d) = a_I T_d \quad (1)$$

where a_I is the rate of phytomer appearence on the primary axis (phytomer °Cd^{-1}).

An end of primary axis development was not included, as this axis does not stop developing in the absence of low-temperature conditions (corresponding to winter) (Lebon *et al.*, 2004).

Secondary axis organogenesis. Four parameters are used to model the development of each secondary axis as a function of its insertion rank (j) on the primary axis as proposed by Pallas *et al.* (2008): a probability of budburst occurrence ($P_{II,j}$), a rate of phytomer appearance according to thermal time ($a_{II,j}$), a duration of development ($D_{II,j}$) and a lag period (°Cd) between the date on which the phytomer on the primary axis bearing the secondary axis appeared and budburst of the corresponding axillary bud ($d_{1,j}$). The number of phytomers [$N_{II,j}(T_d)$] on a secondary axis of insertion rank j at thermal time T_d is described by the following set of equations:

$$\text{if } 0 < T_d < (j/a_I) + d_{1,j} \text{ then } N_{II,j}(T_d) = 0 \quad (2)$$

$$\text{if } (j/a_I) + d_{1,j} \le T_d \le D_{II,j} + (j/a_I) + d_{1,j} \text{ then } N_{II,j}(T_d) = P_{II,j} a_{II,j} [T_d - (j/a_I) - d_{1,j}] \quad (3)$$

$$\text{if } D_{II,j} + (j/a_I) + d_{1,j} < T_d \text{ then } N_{II,j}(T_d) = P_{II,j} a_{II,j} D_{II,j} \quad (4)$$

with $P_{II,j} \in \{0, 1\}$

Model calibration and simulation processes. The values of the parameters used in this model were determined from

measurements on an independent set of plants of the 'Grenache N' cultivar. The plants were grown outdoors in 2006, in pots and in well-watered conditions. In this experiment, daily mean temperature and photosynthetic photon flux density were equal to 23·2 °C and 51·2 mol m^{-2} d^{-1}, respectively. A single vegetative shoot was allowed to develop on these plants, and all the clusters were removed. The values of the parameters differed according to the type of axis (primary and P0, P1–P2 secondary axis), and its insertion rank on the primary axis (Table 1). A regular succession of P0–P1–P2 phytomers on the axis was implemented in the model except for the base of the primary axis (from the first to eighth phytomer) where this regular pattern was not observed (Louarn *et al.*, 2007). Thus, at the base of the primary axis the observed succession was input in the model. For the microclimate variables, only daily mean temperature varied between the different simulations.

'GreenLab-Retroaction' model

General structure and aims. GreenLab is a biomass-driven plant growth model that aims to calculate, at each time step, the total assimilate supply and the total demand from all individual organs. The ratio of the total assimilate supply to the total biomass demand for organ growth has been shown to be a good indicator of trophic competition (Mathieu *et al.*, 2009). Several relationships between trophic competition at the shoot level and axis organogenesis have been described and quantified for grapevine using the deterministic version of GreenLab (fixed organogenesis) (Pallas *et al.*, 2009). These relationships were used in the construction of this plant model in which axis organogenesis is no longer an input variable. The following description of the model focuses particularly on differences with respect to other versions of GreenLab. The main differences between this model and previous GreenLab models concern axis organogenesis, 'reserve' behaviour and biomass production.

Plant topology. The different axes are classified on the basis of their type (k) ($k = 1, 2, 3$ for primary axes and P0 and P1–P2 secondary axes, respectively). The succession of the different types of axis observed on the plant was incorporated into the model. When present, clusters were considered to appear on the first two phytomers on the primary axis (Huglin, 1986).

Primary axis organogenesis and time step of the model. The time step of the model (GC) is one phyllochron of the primary axis. Preliminary studies (Pallas *et al.*, 2010) showed that the development of the primary axis goes on with the same phytomer appearance rate (0·044 phytomer °Cd^{-1}) even in conditions of absence of photosynthetic activity. In this situtation, the same phytomer appearance rate is observed as long as reserve mobilization occurs. In the model, the phytomer production on primary axis is only stopped when the biomass allocated to the vegetative part of the shoot (from reserve mobilization or photosynthesis) is equal to zero. Thus, the duration of the growth cycle is considered to be constant and equal to a constant phyllochron (22·7 °Cd) as long as the biomass allocated to the vegetative part of the shoot (photosynthetic activity and/or reserve mobilization) is non-null. When the biomass allocated to the vegetative part of the shoot is equal to 0, plant development is stopped.

Secondary axis organogenesis. In this model, thermal time determines the maximum rate of development for each axis as the rate of phytomer production on the primary axis. Trophic competition indicates the probability of this potential being reached. In this model axis organogenesis is affected by the ratio of biomass available for non-perennial organs (Q) to the demand for shoot organ expansion and secondary growth (D), hereafter called Q/D ratio. The probability rules associated with Q/D values result in variability in the results of simulations. For each axis, four features are modelled: the probability of budburst (P_b), the duration of the lag period (d_l) (see below), the probability of phytomer production by the axillary meristem (P_p) and the probability of the meristem dying (P_e).

Previous studies have shown that d_l and P_b are not affected by trophic competition (Pallas *et al.*, 2008). The values of these parameters were thus fixed at the start of the simulation, according to the insertion rank of the axis (Table 2).

In previous studies (Pallas *et al.*, 2009), the P0 secondary axes and P1–P2 secondary axes were found to differ in their sensitivity to trophic competition. The rate of phytomer appearance on the different axes remained approximately constant during the development of the axis and depended on trophic competition at the time at which the axis appeared (Louarn *et al.*, 2007). This formalism is implemented in the model by considering P_p to be dependent on the type of

TABLE 1. *Parameter values for the 'thermal time-based' model*

Axis type	Insertion rank (j)	Probability of development ($P_{II,j}$)	Duration of lag period ($d_{l,j}$) (°Cd)	Phytomer appearence rate (a_I, $a_{II,j}$) (phytomer °Cd^{-1})	Duration of development ($D_{II,j}$) (°Cd)
Primary axis	–	–	–	0·044	–
P0 secondary axis	1	0			
	2–4	1	240	0·016	550
	6–15	1	120	0·028	870
	16–30	1	120	0·025	600
	31–45	1	120	0·015	330
	>45	1	120	0·011	52
P1–P2 secondary axis					
	5–15	1	120	0·015	615
	16–30	1	120	0·013	378
	31–45	1	120	0·008	189
	>45	1	120	0·004	52

TABLE 2. *Description of the parameters of organogenesis processes in the 'GreenLab-Retroaction' model, method of calibration and estimated values*

Parameter name	Definition	Units	Method of calibration	Value
Primary axis organogenesis				
GC	Duration of the growth cycle	°Cd	Pallas *et al.*, 2008	23
Secondary axis organogenesis				
$P_b(j)$	Probability of budburst occurrence as a function of insertion rank (j)	–	Pallas *et al.*, 2008	0 for $j = 1$ 1 else
$d_l(j)$	Lag period between phytomer appearance and axis budburst as a function of insertion rank (j)	GC (growth cycle)	Pallas *et al.*, 2008	8 for $j < 5$ 6 else
Probability of stopping development (P_e)				
P0 secondary axis ($k = 2$)	Parameters of the relationships between the probaility of stopping development and Q/D as a function of the number of phytomers on the axis (c)		Model inversion procedure (Pallas *et al.*, 2009)	
$a_e(2, c)$		–	Model inversion procedure (Pallas *et al.*, 2009)	0·091 for $c \leq 5$; 0·012 for $c > 5$
$b_e(2, c)$		–		0·050
P1–P2 secondary axis ($k = 3$)				
$a_e(3, c)$		–		0·143 for $c \leq 5$; 0·102 for $c > 5$
$b_e(3, c)$		–		0·050
Probability of phytomer production (P_p)				
P0 secondary axis ($k = 2$)	Parameters of the relationships between the probability of phytomer production and Q/D		Model inversion procedure, on an independent set of plants	
$c_p(2)$		–		3
P1–P2 secondary axis ($k = 3$)				
$c_p(3)$		–		1·4

$k = 1, 2, 3$ respectively for primary, P0 and P1–P2 secondary axes.

secondary axis (k) and on the value of Q/D when the axillary bud becomes active. The probability of a secondary axis of insertion rank j and of type k [$P_p(j, k, i)$] producing a phytomer during growth cycle i is included in the model.

$$P_p(j, k, i) = c_p(k)\left(\frac{Q(j + d_l)}{D(j + d_l)}\right) \quad (5)$$

with $c_p(k)$ a parameter used to take into account the difference in the sensitivity to trophic competition of P0 and P1–P2 secondary axes, Q the amount of the biomass available for non-perennial organs and D the total demand for shoot organ (petiole, cluster, leaf, internode) expansion and secondary growth.

A consistent correlation between the proportion of secondary axis production ending their development (T_e) and Q/D values at the corresponding growth cycle (i) was observed in previous studies (Pallas *et al.*, 2009). When considering the end of axis development, the sensitivity of secondary axes to trophic competition also depended on the number of phytomers on the corresponding axis (c) and the type of secondary axis (k). Thus, in the model, the probability of a secondary axis of type k, with a number of phytomers c, of insertion rank j, dying during the growth cycle i [$P_e(j, k, c, i)$] is expressed as a function of the predicted proportion of the end of development of secondary axes of type k with a number of phytomers c at growth cycle i [$T_e(k, c, i)$], as follows (Pallas *et al.*, 2009):

$$\begin{cases} \text{if} \quad [1 - T_e(k, c, i)]N_{II}(k, c, i) < N_{II,p}(k, c, i) \\ \quad P_e(j, k, c, i) = \left(\dfrac{N_{II,p}(k, c, i) - N_{II}(k, c, i)[1 - T_e(k, c, i)]}{N_{II,p}(k, c, i)}\right) \\ \text{if } [1 - T_e(k, c, i)]N_{II}(k, c, i) \geq N_{II,p}(k, c, i) \\ \quad P_e(j, k, c, i) = 0 \end{cases} \quad (6)$$

with $N_{II}(k, c, i)$ the total number of secondary axes of type k, with a number of phytomers c at growth cycle i. $N_{II,p}(k, c, i)$ is the potential number of secondary axes calculated by assuming that no new axillary bud died during growth cycle i. With (Pallas *et al.*, 2009):

$$T_e(k, c, i) = 1 - \frac{1}{1 + \exp\left[\dfrac{-\dfrac{Q(i)}{D_p(i)} + a_e(k, c)}{b_e(k, c)}\right]} \quad (7)$$

with $D_p(i)$ the potential demand for biomass, calculated by assuming that no new axillary bud died during growth cycle i.

Photosynthetic production. Biomass production at each growth cycle i [$Q_p(i)$] is incorporated into the model using a Beer-Lambert law formalism, previously applied to grapevine

(Pallas *et al.*, 2009), as follows:

$$Q_p(i) = \mathrm{PPFD}(i) S_P \mathrm{RUE}(i) \left[1 - \exp\left(\frac{-kS(i)}{Sp}\right)\right] \quad (8)$$

with PPFD(i), the photosynthetic photon flux density at each growth cycle (mol m^{-2} GC^{-1}), S_p, the projected leaf area (m^2) (Ma *et al.*, 2008), RUE(i) the radiation use efficiency at growth cycle i (g mol^{-1}) (Monteith *et al.*, 1977), $S(i)$, the total leaf area at growth cycle i (m^2) and k the extinction coefficient for the Beer–Lambert law (Vose *et al.*, 1995).

Radiation use efficiency has been shown to be reduced by water deficit, due to a decrease in CO_2 assimilation (Flexas *et al.*, 2002; Schultz, 2003). In this model, soil water status is determined using the fraction of transpirable soil water (FTSW) defined as the ratio of actual plant-available soil water content to the total plant-available soil water content. The total plant-available water is defined as the difference between soil water content at field capacity and soil water content at 10 % of maximal stomatal conductance (Sinclair and Ludlow, 1986). A function (Lebon *et al.*, 2006) was implemented that modifies at each growth cycle i, the radiation use efficiency RUE(i) as a function of the fraction of transpirable soil water (FTSW(i)].

$$\mathrm{RUE}(i) = \frac{1}{1 + w_1 \exp(w_2[\mathrm{FTSW}(i) + w_3)]} \mathrm{RUE}_{max} \quad (9)$$

with RUE_{max} the maximal value of radiation use efficiency in 'well-watered conditions' and w_1, w_2 and w_3 three parameters of the sigmoid function.

Perennial compartment behaviour. In the model the trunk and roots are considered as a whole and are referred to as the perennial compartment. During the 'heterotrophic' phase of plant development, from budburst to flowering, biomass from the perennial compartment may be mobilized (Koblet and Perret, 1972; Zapata *et al.*, 2004). The initial biomass ($Q_{r,ini}$) of the perennial compartment is input into the model at the start of the simulation procedures. A parameter β_h describes the proportion of the non-structural biomass in the perennial compartment which can be available for shoot development (Keller *et al.*, 1995; Castelan-Estrada, 2001). The time course of biomass mobilization from the perennial compartment is modelled with a beta function [$f_r(i)$] (Yin *et al.*, 2003) and a duration of biomass mobilization [$T_r(i)$]. At each growth cycle i the amount of biomass in the perennial compartement [$Q_r(i)$] is thus calculated as follows:

$$Q_r(i) = Q_r(i-1) - f_r(i)\beta_h Q_{r,ini} \quad (10)$$

During the autotrophic phase of plant development (after flowering; Huglin, 1986) reserve may be both 'stored' and 'mobilized' (Candolfi-Vasconcelos *et al.*, 1994). A parameter $r(i)$ was used to define the threshold level of biomass production below which biomass is mobilized from the perennial compartment. If biomass is stored into the perennial compartment, a parabolic function is implemented to take into account the observed increase in the proportion of biomass allocated to the perennial compartment (Keller *et al.*, 1995; Shipley and Meziane, 2002).

$$Q_r(i) = Q_r(i-1) + a_r Q_p(i)^2 + b_r Q_p(i) \quad (11)$$

with a_r and b_r, two parameters of the parabolic function.

When mobilization occurs, a parameter β_a accounts for the proportion of the perennial compartment biomass that can potentially be mobilized. The fraction of biomass (μ) mobilized from the perennial compartment at each growth cycle is assumed to be constant. Therefore, the total amount of biomass mobilized from the perennial compartment [$Q_{r,a}(i)$] and the total of biomass of the perennial compartment [$Q_r(i)$] can be estimated as follows:

$$Q_{r,a}(i) = \begin{cases} \beta_a Q_r(z)[1 - \mu(i - z + 1)] & \text{if } Q_{r,a}(i-1) > 0 \\ 0 & \text{else} \end{cases} \quad (12)$$

$$Q_r(i) = \begin{cases} Q_r(i-1) - \mu\beta_a Q_r(z) & \text{if } Q_{r,a}(i-1) > 0 \\ Q_r(i-1) & \text{else} \end{cases} \quad (13)$$

with z, the growth cycle at which mobilization begins.

Biomass allocation to the non-perennial organs. The combination between photosynthetic production (Q_p) and the perennial compartment behaviour allows the part of biomass allocated to the shoot [$Q(i)$] to be calculated. A parameter α has been incorporated into the model to take into account the proportion of the biomass mobilized from the perennial compartment and actually converted into biomass for shoot development (Castelan-Estrada, 2001).

During the 'heterotrophic' phase of plant development:

$$Q(i) = Q_p(i) + \alpha f_r(i)\beta_h Q_{r,ini} \quad (14)$$

During the 'autotrophic' phase of plant development:

$$\begin{cases} \text{if } Q_p(i) > r(i) \\ \quad Q(i) = (1 - b_r)Q_p(i) - a_r Q_p(i)^2 \\ \text{if } Q_p(i) \le r(i) \\ \quad Q(i) = \begin{cases} Q_p(i) + \alpha\mu\beta_a Q_r(z) \\ 0 \qquad\qquad \text{else} \end{cases} \end{cases} \quad (15)$$

Biomass allocation between non-perennial organs. In GreenLab, biomass allocation processes are organized into two phases: a phase of biomass allocation to each growth process (organ expansion, and secondary growth) and a phase of allocation to the different organs (Letort *et al.*, 2008; Mathieu *et al.*, 2009).

The demand for organ expansion is calculated as previously proposed in GreenLab (Yan *et al.*, 2004). Each organ ($o = b, e, p, c$ for blade, internode, petiole and cluster, respectively) on each type of axis (k) is defined using a sink strength [$P_o(k)$], and a beta law function [$f_o(n)$] (Yin *et al.*, 2003; Yan *et al.*, 2004) (with three parameters: a_o, b_o and $T_{exp,o}$) depending on the type of organ (o) and on the time after organ emergence ['chronological age' (n)]. Clusters undergo two phases of development: from flowering (stage 23 according to the

modified Eichorn and Lorenz scale; Coombe, 1995) to veraison (stage 35), and from veraison to maturity (stage 39) (Coombe, 1976). Therefore two organs ($o = c_1$ and c_2 for clusters between flowering and veraison and from veraison to maturity, respectively), were implemented with their own associated sink strengths and beta functions. The total demand for organ expansion at growth cycle i [$D_{exp}(i)$] is thus defined as proposed by Yan *et al.* (2004):

$$D_{exp}(i) = \sum_k \sum_o P_o(k) \sum_n f_o(n) N_o(n, k, i) \quad (16)$$

where $N_o(n, k, i)$ is the total number of organs of type o, of an axis of type k and chronological age n in the plant at growth cycle i.

The total demand for secondary growth at growth cycle i [$D_s(i)$] is incorporated into the model, as proposed by Letort (2008) as a function of total leaf area $S(i)$ and using a constant sink strength (P_s).

$$D_s(i) = P_s S(i) \quad (17)$$

The total biomass demand ($D(i)$] of the shoot at each growth cycle i can be expressed as:

$$D(i) = D_{exp}(i) + D_s(i) \quad (18)$$

The proportion of the biomass allocated to organ expansion (Q_{exp}) and secondary growth (Q_s) at each growth cycle is assumed to depend only on the relative demand for each growth process, as proposed by Letort *et al.* (2008) or Mathieu *et al.* (2009):

$$Q_{exp}(i) = D_{exp}(i) \frac{Q(i)}{D(i)} \quad (19)$$

$$Q_s(i) = D_s(i) \frac{Q(i)}{D(i)} \quad (20)$$

The biomass allocated to each organ for its expansion [$\Delta q_o(n, k, i)$] is given by:

$$\Delta q_o(n, k, i) = P_o(k) f_o(n) \frac{Q(i)}{D(i)} \quad (21)$$

The biomass allocated to the secondary growth of each internode is defined according to a previously described formalism (for a complete description, see Letort *et al.*, 2008), using a flexible submodel with two modes of allocation, one based on the 'pipe model' theory (Shinozaki *et al.*, 1964; Mäkela, 1986) and the other based on uniform allocation from the 'common assimilate pool' (Heuvelink, 1995). The two models are combined with a coefficient λ in [0 ; 1].

The individual leaf area [$S_j(i)$] at each growth cycle is calculated, using a specific leaf weight (SLW(i)], which is a function of the photosynthetic photon flux density (PPFD(i)] (Meziane and Shipley, 1999):

$$S_j(i) = \frac{q_{l,x}(i)}{SLW(i)} \quad (22)$$

with

$$SLW(i) = a_l PPFD_m + b_l \quad (23)$$

where $q_{l,x}(i)$ is the biomass of the blade of the leaf x at growth cycle i and a_l, b_l two parameters of the linear function. In the model the amount of photosynthetic radiation for the calculation of SLW was considered to be equal to its mean value ($PPFD_m$).

Internode shape is calculated from flexible allometric relationships between internode mass, length and diameter. Allometric relationships for the internodes were directly estimated on the observed plants, for each set of experimental conditions.

Model calibration. The information used to set the parameter values was obtained from three sources: (1) the GreenLab model inversion procedure applied to an independent set of plants; (2) measurements; (3) published results (Tables 2–4).

The GreenLab inversion procedure has been described elsewhere and can be used to estimate hidden parameters of the GreenLab model from observed data (Guo *et al.*, 2006; Letort *et al.*, 2008). This procedure was performed on an independent set of plants of 'Grenache N', grown outdoors in 2006, in large pots and in well-watered conditions. A single vegetative shoot was allowed to develop on these plants. On a first set of plants, all the clusters were removed while the plants of another set carried two and six clusters. Plants were grown in the same microclimatic conditions as for the thermal time-based model. The results of the fitting procedures on these plants were presented in a previous article (Pallas *et al.*, 2009). This optimization procedure made it possible to estimate the parameters of the relationships between the probability of phytomer production, axis death and Q/D. This procedure was also used to estimate the sink strength of each organ (blade, petiole, internode and cluster) and their associated beta-law functions. The values of RUE_{max} and of the extinction coefficient for the Beer–Lambert law (k) were estimated using this inversion procedure using the set of plants with all the clusters removed. The model inversion procedure was also used to estimate the values of the parameters of the beta-law function for biomass mobilization from the perennial compartment during the heterotrophic phase ($a_{r,i}$, $b_{r,i}$) of shoot development (eqn 10). The reserve mobilization parameters during the autotrophic phase [β_a, $r(i)$, μ, α] were calculated by estimating the maximum level of biomass mobilization from the perennial compartment. These estimations were made on plants without photosynthetic activity that had been grown under a polyester shelter (autumn 2008) or fully defoliated (2008) (see Pallas *et al.*, 2009). The parameters for biomass storage in the perennial compartment (a_r, b_r) were estimated in the three experiments described below and in another two experiments on 'Grenache N' plants grown outdoors in pots during the summers of 2006 (Pallas *et al.*, 2008) and 2007 (Pallas *et al.*, 2010). The values of these parameters (a_r, b_r) were estimated by calculating differences in the root : shoot ratio as a function of plant biomass production. The initial part of mobilizable biomass in the perennial compartment (β_h) was determined on these same set of plants as the difference between the dry weight of the perennial

TABLE 3. *Description of the parameters (biomass production and allocation) for the 'GreenLab-Retroaction' and 'Water-GreenLab' model, method of calibration and estimated values*

Parameter name	Definition	Units	Method of calibration	Value
Biomass production				
RUE_{max}	Radiation use efficiency (Monteith, 1977)	g mol^{-1}	Model inversion procedure on a independant dataset (Pallas *et al.*, 2009)	0·52
Sp	Projected leaf area (Ma *et al.*, 2008)	m^2		0·4
k	Extinction coefficient of the Beer–Lambert Law (Vose *et al.*, 1995)	–		0·80
Water deficit impact on biomass production				
w_1	Coefficient of the function : RUE = f(FTSW)	–	Lebon *et al.*, 2006	6·20
w_2		–		−6·36
w_3		–		0·14
Perennial compartment behaviour				
'Heterotrophic phase'				
$Q_{r,ini}$	Initial biomass of the perennial compartment	g	Measurements	≈30 (depending on experiment)
β_h	Proportion of non-structural biomass of the perennial compartment	–		0·08
$a_{r,i}$	Beta law function parameters of reserve mobilization function (fr)	–	Model inversion procedure (Pallas *et al.*, 2009)	2
$b_{r,i}$				10
'Autotrophic phase'				
Reserve storage		–	Measurements on independant sets of plants	
a_r	Coefficients used to estimate the part of photosynthetic biomass allocated to the perennial compartment	–		0·0048
b_r		–		0·159
Reserve mobilization				
$r(i)$	Threshold of biomass production for biomass mobilization	g		0
β_a	Proportion of non-structural biomass of the perennial compartment	–		0·20
μ	Fraction of reserve biomass mobilized from the perennial compartment	–		0·025
α	Coefficient of conversion between perennial compartment and shoot biomasses	–		0·15

compartment at budburst and at flowering time divided by the whole perennial compartment biomass at budburst. The duration of organ expansion ($T_{exp,o}$) was estimated by direct measurements on plants grown outside in 2007. The parameters of SLW variation as a function of the photosynthetic flux density were estimated directly on the set of plants subsequently simulated and in two experiments carried out during the summers of 2006 and 2007.

Published data were also used to estimate the values of the parameters concerning the effect of FTSW on RUE (a_w, b_w, c_w), for the probability of budburst occurrence (P_b) and for budburst date (d_1).

Simulation procedure and input parameters. The mean temperature, FTSW and PPFD were the microclimate parameters that varied between experiments. The total dry weight of the trunks and roots was determined before budburst on a set of plants in each experiment to determine the initial dry weight of the perennial compartment ($Q_{r,ini}$). This parameter $Q_{r,ini}$ was also considered as an input parameter. As the model is not deterministic, 50 repetitions of the simulation procedure were performed to calculate the mean values.

'Water-GreenLab' model

Underlying concepts. Many authors have observed a decrease in axis organogenesis in conditions of water shortage, independently of any decrease in photosynthetic activity (Davies and Zhang, 1991; Tardieu *et al.*, 1999). In the 'GreenLab-Retroaction' model, FTSW modifies plant development by acting only on photosynthetic activity and Q/D ratio (eqn 9). The aim of the 'Water-GreenLab' model is to simulate axis organogenesis as a function of soil water content and Q/D ratio. The biomass allocation formalisms of the 'GreenLab-Retroaction' model are maintained unchanged in this model. Therefore only the formalisms driving axis organogenesis that differ between these two models are described below.

Axis organogenesis. Previous studies have shown that the rate of phytomer appearence on the primary axis is affected by water deficit. This modifies the duration of the growth cycle (GC), defined as the phyllochron of the primary axis (Lebon *et al.*, 2006):

$$GC = (1/a_I)(1 + a_{w,I}\exp[b_{w,I}(FTSW(t) + c_{w,I})]) \quad (24)$$

with FTSW(t) the fraction of transpirable soil water at time t, $a_{w,I}$, $b_{w,I}$ and $c_{w,I}$ three parameters, and a_I the phytomer

TABLE 4. *Description of the parameters (biomass allocation between non-perennial organs and allometric relationships) for the 'GreenLab-Retroaction' and 'Water-GreenLab' models, method of calibration and estimated values*

Parameter name	Definition	Units	Method of calibration	Value*
Sink strengths [$P_o(k)$]		–		
Blade [$P_b(k)$]	Sink strength of the different organs as a function of physiological age (k) (Yan *et al.*, 2004)		Model inversion procedure on an independent dataset (Pallas *et al.*, 2009)	1 for $k = 1$, 0·6 for $k = 2$, 0·4 for $k = 3$
Internode [$P_e(k)$]				0·86 for $k = 1$ 0·61 for $k = 2$ 0·43 for $k = 3$
Petiole [$P_p(k)$]				0·12 for $k = 1$ 0·05 for $k = 2$ 0·04 for $k = 3$
Cluster 1 [$P_{c1}(k)$]				6
Cluster 2 [$P_{c2}(k)$]				61
Sink variation parameter				
Beta law function coefficient (a_o; b_o)		–		
Blade (a_b; b_b)	Parameters of the sink function variation (Yan *et al.*, 2004)			(2·5; 3·5)
Internode (a_e; b_e)				(2; 4·5)
Petiole (a_p; b_p)				(2·5; 2·5)
Cluster 1 (a_{c1}; b_{c1})				(2; 3·5)
Cluster 2 (a_{c2}; b_{c2})				(2·5; 6)
Duration of development ($T_{exp,o}$)		GC (growth cycle)		
Blade	Duration of organ expansion (Yan *et al.*, 2004)		Measurements on an independent set of plants	12
Internode				12
Petiole				16
Cluster 1				28
Cluster 2				21
Allometric relationships		–		
a_l	Parameters of the equation SLW = a_l. PAR + b_l (SLW, mg.cm^{-2})		Measurements ($r^2 = 0{\cdot}83$, RRMSE = 20·2 %)	0·087
b_l		–		1·33
Secondary growth				
P_s	Constant sink strength for secondary growth	m^{-2}	Model inversion procedure on an independent dataset (Pallas *et al.*, 2009)	7
λ	Coefficient of partitioning between the 'Pressler' and the 'common pool' allocation mode (Letort *et al.*, 2008)	–		0·6

*$k = 1$, 2, 3, respectively, for primary, P0 and P1–P2 secondary axes.

appearance rate on the primary axis in well-watered conditions.

Water deficit modifies the rate of phytomer appearance on the secondary axis without affecting the duration of development (Lebon *et al.*, 2006). Moreover, the different secondary axes (P0 or P1–P2) are affected to similar extents by water deficit. The effect of soil water deficit on $P_p(j, k, i)$ is incorporated into the model as proposed by Lebon *et al.*, (2006) (Fig. 1):

$$P_p(j,k,i) = \left(\frac{1}{1 + a_{w,II}\exp[b_{w,II}(\mathrm{FTSW}(i) + c_{w,II})]}\right) c_p(k) \times \left(\frac{Q(j+d_l)}{D(j+d_l)}\right) \quad (25)$$

with $a_{w,II}$, $b_{w,II}$ and $c_{w,II}$ three parameters of the sigmoid equation.

Model calibration, simulation procedure and sensitivity analysis. Parameter values were estimated from the data presented in the study by Lebon *et al.* (2006) (Table 5). The input parameters in the various simulations were the microclimate data (T °C, PPFD and FTSW) and initial perennial compartment biomass ($Q_{r,ini}$). As the model is not deterministic, 50 repetitions of the simulation procedure were performed to calculate mean values. A sensitivity analysis, in which each input variable was varied separately, was carried out to evaluate the relative impact of different input variables on axis organogenesis, biomass allocation and production.

Three-dimensional representations of plants

Three-dimensional representations of the simulated plants, on which only the aerial parts of the plants were drawn, were constructed to illustrate the results of simulations. Empirical allometric relationships were established to link internode dry weights to internode length and diameter (see below). The phyllotaxy of the leaf and the divergence angle were fixed to 180° and 30°, respectively (Huglin, 1986).

Model validations

Experimental design. Six experiments were carried out at the Montpellier-SupAgro Campus (43°38′N, 3°53′E) from 2000

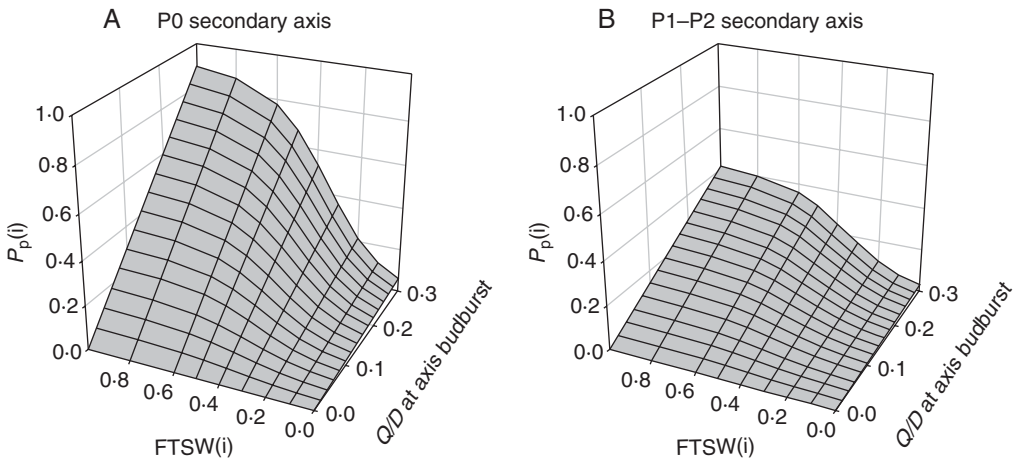

FIG. 1. Calculation of the probability of producing a phytomer at each growth cycle, for P0 (A) and P1–P2 (B) secondary axes in the 'Water-GreenLab' model. For each axis, the probability of producing a phytomer at growth cycle *i* is calculated from the *Q*/*D* ratio at the start of axis development and FTSW at growth cycle *i*.

TABLE 5. *Description of the parameters used to estimate the probability of producing a leaf on secondary axes and the duration of the growth cycle as a function of FTSW in the 'Water-GreenLab' model, method of calibration and estimated values*

Parameter name	Definition	Unit	Method of calibration	Value
a_I	Maximal phytomer appearence rate on the primary axis	Phytomer °Cd^{-1}	Lebon *et al.*, 2006	0·044
$a_{w,I}$	Parameters of the relationships between the duration of the growth cycle and FTSW values	–	Lebon *et al.*, 2006	11·80
$b_{w,I}$		–		−7·41
$c_{w,I}$		–		0·18
$a_{w,II}$	Parameters of the relationships between the probability to produce a leaf and FTSW values	–	Lebon *et al.*, 2006	1·73
$b_{w,II}$		–		−7·51
$c_{w,II}$		–		−0·28

to 2008 (Table 6). In each experiment, 3-year-old grapevine (*Vitis vinifera*) plants of the 'Grenache N' cultivar grafted onto Fercal rootstocks were studied. In expts 1–5, 23, 22, 20, 20 and 18 plants were grown, respectively, and the data from expt 6 were published by Lebon *et al.* (2006). Plants were grown outdoors in expts 1, 2 and 6, and in a greenhouse in expts 3, 4 and 5. In expt 5, plants were placed under a polyester shelter, from 600 °Cd after budburst to the end of the experiment. This experimental design resulted in a broad range of PPFD values, from 54·2 mol m^{-2} d^{-1} to 0.

In all experiments, plants were grown in PVC pots filled with a 1 : 1 : 1 (v/v/v) mixture of topsoil, sand and organic compost. Plants were grown in small pots in expts 1–5 (0·0069 m^3) and in large pots in expt 6 (0·05 m^3). Because the plants were frequently watered with an automatic irrigation system, small pots were used in expts 1–5, but, in expt 6, as plants were manually watered daily, large pots were used to avoid rapid drying out of the growing medium. Fertilizer applications were managed so as to avoid mineral deficiency. In expts 1–5, FTSW was maintained above 75 % of pot capacity, corresponding to 'well watered' conditions for grapevine (Lebon *et al.*, 2006). In expt 6, three levels of FTSW were imposed from 350 °Cd after budburst to the end of the experiment (FTSW = 0·89, 0·47 and 0·09). Depending on the agronomic indicators (Carbonneau *et al.*, 2007), FTSW values 1–0·65 correspond to 'well watered' conditions, FTSW values 0·65–0·3 correspond to 'moderate' soil water deficit, and FTSW values below 0·3 correspond to severe water deficit.

In expts 1–6, plants were pruned to a single shoot at the 'five separated leaves' stage (stage 12; Coombe, 1995). This shoot was trained vertically and allowed to continue its vegetative development. Two cluster-load treatments were applied. Inflorescences were removed for the 'control' treatments (expts 1–6), whereas, for the 'control-clusters' treatments (expt 1) two clusters were retained (stage 39).

Plant measurements. For each treatment (except for expt 6), four plants were harvested at four stages of development. The first harvest was performed just before budburst, to evaluate the initial weight of the perennial compartment. The second, third and fourth harvests were carried out approx. 550 and 800 and 1150 °Cd, respectively, after budburst. The dry weight of each organ on the primary axis (leaf, internode and cluster) was determined. For each secondary axis, the total dry weight of each type of organ (leaf and internode) was also determined. The total dry weight of clusters and perennial compartment (trunk and roots) was also determined. In

TABLE 6. *Environmental conditions in the various experiments used for model validation*

Expt	Date	Location	Daily mean temperature (°C)	Daily cumulative PPFD (mol m^{-2} d^{-1})	Mean FTSW
1	May–August 2008	Outdoors	24·2	51·2	–
2	July–September 2008	Outdoors	22·6	39·1	–
3	March–June 2008	Greenhouse	20·1	12·9	–
4	September–December 2008	Greenhouse	20·6	7·0	–
5*	March–June 2008	Greenhouse-shelter	22·1	0·0	–
6 (Lebon *et al.*, 2006)	Summer 2000	Outdoors	23·4	54·2	0·89; 0·47; 0·09

* In this table, in expt 5, the data represent the microclimate conditions from 600 °Cd to maturity for plants grown during this period. Before 600 °Cd, plants were grown in the same microclimate conditions as for expt 3.

TABLE 7. *Observed and simulated values ('thermal time-based' and 'GreenLab-Retroaction' models) of the number of phytomers on the primary and secondary axes at 1200 °Cd after budburst*

		Primary axis			Secondary axis		
Expt	Treatment	Mean observed value	Simulated value with the 'thermal-time' model	Simulated value with 'GreenLab-Retroaction'	Mean observed value	Simulated value with the 'thermal-time' model	Simulated value with 'GreenLab-Retroaction'
1	'Control-clusters'	53·1[a]	52·8	53	318[a]	301	282
1	'Control'	53·6[a]	52·8	53	331[a]	301	319
2	'Control'	51·6[a]	52·8	53	260[b]	301	251
3	'Control'	52·6[a]	52·8	53	105[c]	301	118
4	'Control'	50·7[a]	52·8	53	66[cd]	301	84
5	'Control'	31·2[b]	52·8	28	45[d]	301	38
	RRMSE		20·1 %	3·3 %		97·4 %	10·8 %

* Values followed by different letters were significantly different ($P < 0·05$).
The simulation results were calculated with 50 repetitions of the simulation procedure.

expt 6 (Lebon *et al.*, 2006), no data concerning changes in the dry weights of the organs were available. The initial biomass of the perennial compartment ($Q_{r,ini}$) was therefore considered to be the mean of the values obtained in the other experiments.

From budburst to 799 °Cd (expt 6) or 1200 °Cd (expts 1–5), the number of phytomers on the various axes and the succession of axis types (P0–P1–P2) were recorded twice weekly.

Statistical analysis

The ANOVA procedure of Statistica 6·0 (Statsoft, Tulsa, OK) was used to test for significant differences between treatments and experiments. Newman–Keul's test was used as a *post hoc* test for pairwise comparisons.

The criterion used to evaluate the goodness of simulation was the root mean square error (RMSE):

$$\mathrm{RMSE} = \sqrt{\frac{\sum_{i=1}^{N} (X_i - Y_i)^2}{N}} \tag{26}$$

with X_i the observed values, Y_i the corresponding simulated results and N the number of observations.

The relative RMSE (RRMSE) was also calculated.

$$\mathrm{RRMSE} = \frac{\mathrm{RMSE}}{\bar{Y}} \tag{27}$$

where $\bar{Y}$ is the mean value of all observed data.

RESULTS

Experimental results in well-watered conditions

The number of phytomers on the primary axis at 1200 °Cd was similar in expts 1–4, but was significantly lower in expt 5 (Table 7). Significant differences in the number of phytomers on secondary axes were observed between experiments. For this variable, the experiments could be ranked in descending order as follows: expt 1 > expt 2 > expt 3 > expt 4 >expt 5. No significant difference was observed between the 'control' and 'control-clusters' treatments in expt 1. The changes in secondary axis development according to the insertion rank, axis type and environmental conditions are shown in Fig. 2 for expts 1 and 3 (not shown for expts 2, 4 and 5). In each experiment the number of phytomers on P0 secondary axes was significantly higher than the number of phytomers on P1–P2 secondary axes. For the outside experiments (expt 1, Fig. 2A and B; not shown for expt 2), the number of

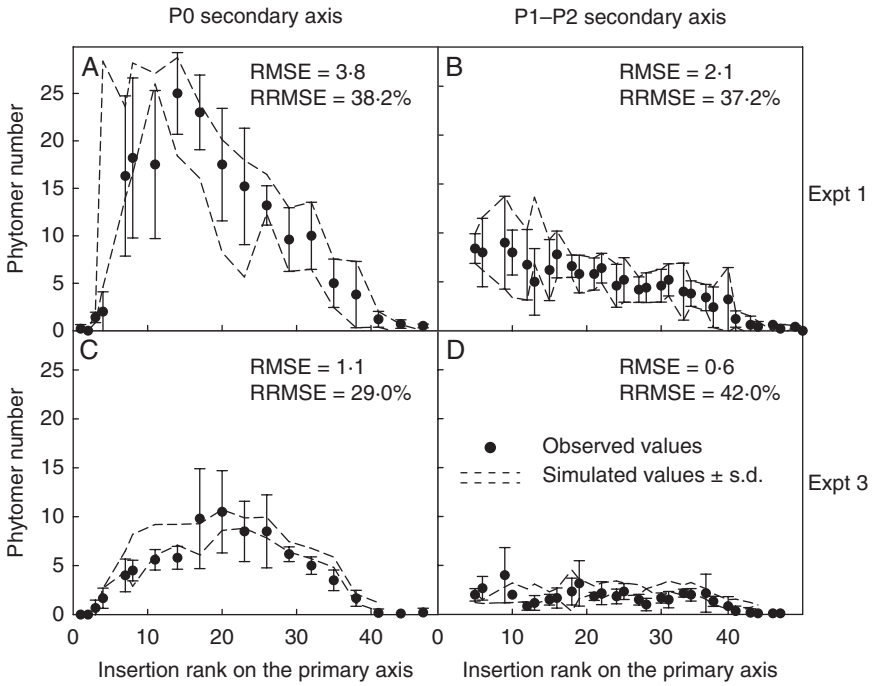

FIG. 2. Observed (closed circles) and simulated (dashed lines) values for the final number of phytomers on each secondary axis at 1200 °Cd. The simulated values were calculated with the 'GreenLab-Retroaction' model. Values are presented as a function of insertion rank and secondary axis type, for 'control' treatments of expts 1 (A, B) and 3 (C, D). (A) and (C) show the mean number of phytomers for P0 secondary axes and (B) and (D) show the mean number of phytomers for P1–P2 secondary axes. In expt 1, plants were grown outside, whereas in expt 3, plants were grown in a greenhouse. As the 'GreenLab-Retroaction' model is not deterministic, the space between the two lines represents the simulated values ± the standard deviation of the simulation (50 repetitions of the simulation procedure). Bars indicate the s.d. of the observed values.

phytomers on the P0 secondary axis increased from the bottom to approximately phytomer 14 and then gradually decreased. The maximal number of phytomers was equal to 25·0 phytomers at the insertion rank 14 in expt 1 (21·3 phytomers at the insertion rank 11 in expt 2). Concerning the P1–P2 secondary axes, in expt 1 the maximal number of phytomers was equal to 9·0 phytomers at the insertion rank 9 (7·5 for insertion rank 9 in expt 2). Above this rank the number of phytomers for the P1–P2 secondary axes gradually decreased. For the greenhouse experiments (expts 3 and 4; not shown for expt 4), the variability in the number of phytomers between each secondary axis was lower than for the outside experiments. In expt 3 the maximal number of phytomers on P0 secondary axis was equal to 10·5 at insertion rank 20 (6·1 at insertion rank 17, in expt 4 not shown) and was equal 4·5 at insertion rank 19 (2·1 at insertion rank 21, in expt 4 not shown) for P1–P2 secondary axes. Below the shelter, the maximal number of phytomers was equal to 4·2 for the P0 secondary axis at insertion rank 11.

Plant development modelling in well-watered conditions

The thermal time-based model was highly consistent with the observed values for primary axis organogenesis in expts 1–4 (mean RRMSE = 7·7 %), but was not appropriate for the plants grown under the shelter (expt 5) (Table 7). The model simulated the number of phytomers on secondary axes poorly, if the entire dataset was considered (mean RRMSE = 97·4 %). However, the model adequately simulated secondary axis organogenesis if plants were grown in the same radiation conditions used for model calibration (high PPFD values, expts 1 and 2).

The 'GreenLab-Retroaction' model was highly consistent with the observed values for the number of phytomers on primary and secondary axis at 1200 °Cd (Table 7), for all experiments and treatments (RRMSE = 3·3 and 10·8 %, respectively, for primary and secondary axes). This model predicted a slightly smaller number of phytomers on secondary axes for the 'control-clusters' treatment (282 phytomers) than for the control treatment (319 phytomers). This difference in the number of predicted phytomers is due to the higher level of trophic competition (lower Q/D) in the presence of clusters. The highest level of trophic competition was mainly observed after 'véraison' which corresponds to the period where the highest rate of cluster development can be observed (data not shown). Nevertheless, this difference was not significant in experimental conditions.

The 'GreenLab-Retroaction' model reproduced the spatial distribution of the phytomers at 1200 °Cd well for the 'control' treatments in expts 1 and 3. The RRMSE for the number of phytomers on each secondary axis as a function of insertion rank was 36·2 % if both experiments were considered (Fig. 2). The model is not deterministic, so the output values generated by the model vary between simulations. For 50 repetitions of the simulations, the model predicted total phytomer numbers with a standard deviation of 12·6 and 6·1 phytomers in expts 1 and 3, respectively. At the axis level, the standard deviations of the simulation were 3·3 and 1·6 phytomers for the P0 secondary axes in expts 1 and 3, respectively, and 1·8 and 0·8 phytomers, respectively, for P1–P2 secondary axes.

The ability of the 'GreenLab-Retroaction' model to simulate total leaf area, total dry mass accumulation, and perennial compartment and cluster dry masses was assessed (Table 8). Significant differences ($P < 0{\cdot}001$) between experiments were observed for these five variables at 1150 °Cd. The experiments could be ranked for these variables as follows: expt 1 > expt 2 > expt 3 > expt 4 > expt 5. The model simulated this pattern well, and the variable with the lowest RRMSE was total dry mass (19·7 %), that with the highest RRMSE being perennial compartment dry mass (25·1 %). These values of RRMSE are close to the value of the coefficient of variation for the observed data (approx. 0·25). The model also reproduced the temporal variations of these variables for the whole dataset (Fig. 3) (data not shown for expts 2 and 4). For the dynamics of biomass production and partitioning and for total leaf area development, mean RRMSE ranged from 11·4 and 18·1 %. The visualization procedure of the model allows a global overview of the impact of environmental variables on the simulations of axis organogenesis to be presented using the 'GreenLab-Retroaction' model (Fig. 4). The simulation of the plants grown in the greenhouse did not give smaller plants than those grown outdoors, but gave plants with fewer phytomers.

Experimental results in fluctuating soil water conditions

A significant decrease in axis organogenesis, on both primary and secondary axes, was observed 799 °Cd after budburst in severe water-deficit conditions (FTSW = 0·09) (Table 9). In situations of moderate water deficit (FTSW = 0·47), only the number of phytomers on secondary axes decreased significantly.

Plant development modelling in fluctuating soil water conditions

The simulations of primary axis organogenesis generated by the 'GreenLab-Retroaction' model were consistent with observed data for FTSW values of 0·89 and 0·47, but overestimated the number of phytomers when the FTSW was 0·09 (Table 9). Conversely, the 'Water-GreenLab' model simulated variation in primary axis organogenesis well (RRMSE = 5·2 %). For secondary axis organogenesis, both models tended to underestimate the number of phytomers on secondary axes at 799 °Cd, for a FTSW of 0·89, but the 'Water-GreenLab' model seems to simulate the decrease in axis organogenesis with decreasing soil water content more effectively. Indeed, it was observed that there were 29 % and 78 % fewer phytomers on the secondary axes at FTSW values of 0·47 and 0·09, respectively, than at an FTSW value of 0·89. The 'Water-GreenLab' model predicted 21 % and 81 % decreases in the number of phytomers on secondary axes, and the 'GreenLab-Retroaction' predicted decreases of 2 % and 50 %. The 'Water-GreenLab' predicted changes in the allocation coefficients between perennial compartment and annual vegetative shoot according to soil water content. The part of biomass allocated to the perennial compartment at 799 °Cd after budburst was, respectively, equal to 23·1, 24·2 and 14·9 % of the total biomass supply, respectively, for FTSW = 0·89, 0·47 and 0·09. Figure 5 illustrates the results of the simulation of plant development performed with the 'Water-GreenLab' in fluctuating soil water conditions.

Then the sensitivity of the 'Water-GreenLab' model to FTSW was thoroughly tested to explore its behaviour and the coherence of its response (Fig. 6). In situations of moderate water deficit ($0{\cdot}3 < \text{FTSW} < 0{\cdot}65$), this model assumes that axis organogenesis is the most strongly affected variable, with cluster dry mass assumed to be the least affected variable (−48 and −9 % for FTSW = 0·4, for axis organogenesis and cluster dry mass, respectively). The output of the model indicates that the decrease in axis organogenesis is more marked than that in total dry mass in situations of moderate soil water deficit. In situations of severe water deficit ($\text{FTSW} < 0{\cdot}3$) cluster dry mass is more sensitive to FTSW than in situations of moderate soil water deficit, and perennial compartment biomass is the most strongly affected variable.

DISCUSSION

A modelling approach to increase the domain of validity of models based on source–sink relationships

Three different models have been presented here: the 'thermal time', 'GreenLab-Retroaction' and 'Water-GreenLab' models. The thermal time-based model is often used in agronomic contexts to estimate the potential number of phytomers on each axis (Pallas *et al.*, 2008). The other two models are innovative and based on GreenLab formalisms for biomass allocation. The combination of the 'GreenLab-Retroaction'

TABLE 8. *Observed and simulated values ('GreenLab-Retroaction' model) for total leaf area, total dry mass and reserve dry mass at the end of the experiment (approx. 1150 °Cd)*

		Leaf area (m^2)		Total dry mass (g)		Perennial compartment dry mass (g)	
Expt	Treatment	Observed	Simulated	Observed	Simulated	Observed	Simulated
1	'Control-clusters'	2·63[a]	2·92	406[a]	429	131[a]	152
1	'Control'	2·79[a]	3·28	373[a]	437	123[a]	146
2	'Control'	2·01[b]	2·55	251[b]	313	86[b]	114
3	'Control'	1·45[c]	1·81	181[c]	158	59[c]	54
4	'Control'	1·05[cd]	1·21	136[d]	101	46[c]	39
5	'Control'	0·60[d]	0·39	59[e]	38	25[d]	23
RRMSE			24·4 %		19·7 %		25·1 %

Values followed by different letters were significantly different ($P < 0{\cdot}05$).
The simulation results were calculated with 50 repetitions of the simulation procedure.

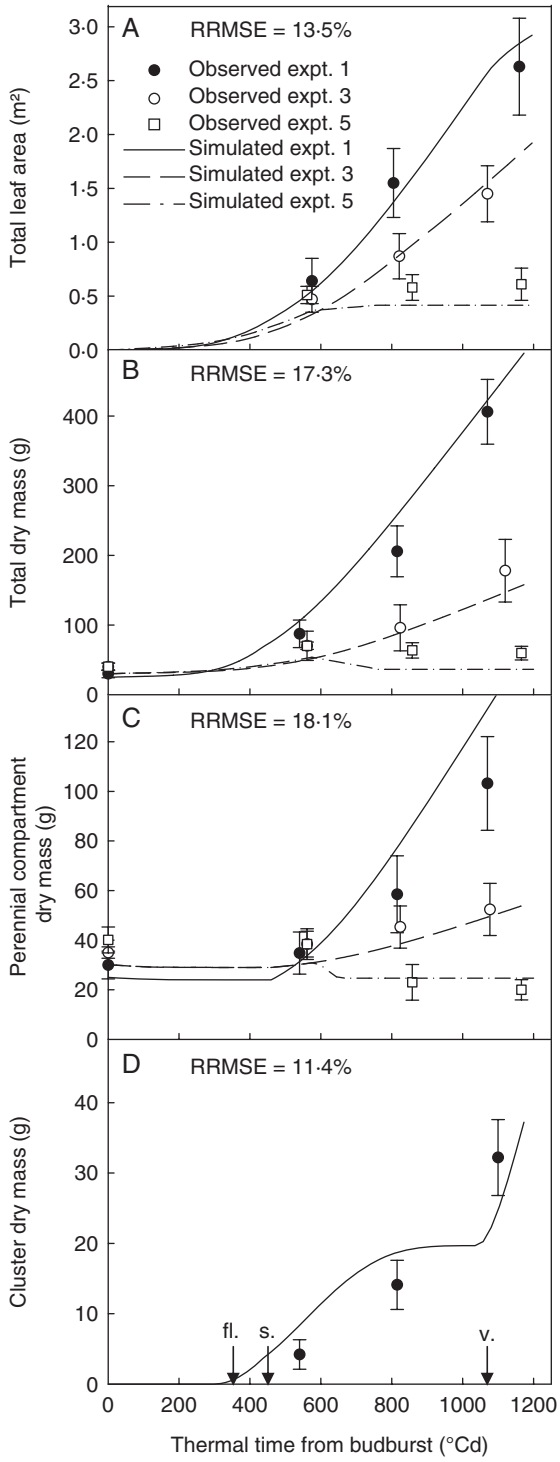

FIG. 3. Observed (symbols) and simulated (lines) values for leaf area (A), total dry mass (B), perennial compartment dry mass (C) and cluster dry mass (D) according to thermal time from budburst for the plants of the 'control-clusters' treatment in expt 1 and the 'control' treatment in expts 3 and 5. Arrows in (D) indicate the date of the main phenological stages [fl., flowering (stage 23 according to the modified Eichorn and Lorenz scale; Coombe, 1995); s., setting (stage 27); v., veraison (stage 35)]. The simulated values were calculated with the 'GreenLab-Retroaction' model. Values are the mean of the 50 repetitions of the simulation procedure. Bars indicate the s.d. of the observed values.

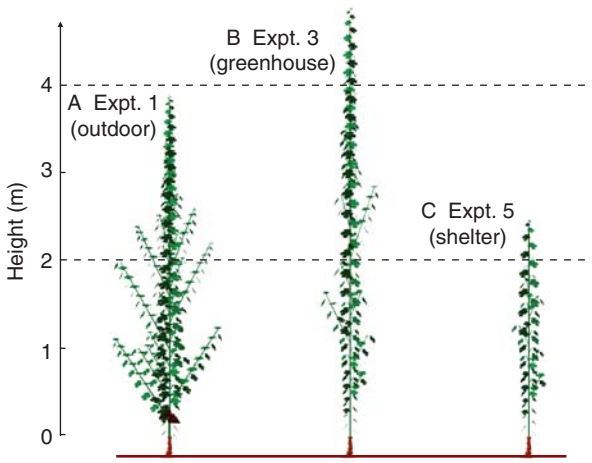

FIG. 4. Visualization of simulation results ('GreenLab-Retroaction' model), 1200 °Cd after budburst, with input parameters corresponding to the microclimate conditions in expts 1 (A), 3 (B) and 5 (C). For expt 1, simulations were performed with the plants of the 'control-clusters' treatment and, in expts 3 and 5, simulations were performed on 'control' treatments.

and 'Water-GreenLab' models is an attempt to construct a functional–structural plant model based on source–sink relationships and on GreenLab formalisms. These models make it possible to simulate the axis organogenesis of a plant with a complex branching system in conditions of fluctuating temperature, solar radiation and soil water content.

The inclusion in the 'GreenLab-Retroaction' model of several relationships linking axis organogenesis and trophic competition improved the results of model simulations for secondary axis organogenesis in environments in which solar radiation levels fluctuated compared with the thermal time based model. Using this model the RRMSE was divided by a factor 9 compared with the simulations using the model based only on thermal time (Table 7). This is of considerable interest because secondary axis organogenesis is highly plastic and appears to be the principal process underlying leaf area variation (Lebon *et al.*, 2004; Pallas *et al.*, 2010). For the primary axis, the 'GreenLab-Retroaction' only improved the results of model simulations when the photosynthetic activity of the plants was equal to 0.

The 'Water-GreenLab' model further improved simulations of axis organogenesis for both primary and secondary axes in the presence of a water deficit. This model decreased the RRMSE by a factor of 2–5 compared with the 'GreenLab-Retroaction' model (Table 9). This finding is of considerable importance in the development of models for grapevine, because soil water deficit is the main abiotic stress in vineyard conditions. Finally, this 'Water-GreenLab' model reproduced an observed pattern with potential consequences for agronomic practice (Fig. 6). In a situation of moderate soil water deficit, it reproduced a large decrease in axis organogenesis which was not correlated to the biomass production. This lack of connection between axis organogenesis and photosynthetic activity tends to promote cluster growth. Although this trend has been observed in agronomic conditions (Carbonneau *et al.*, 2007), this is the first time that it has been quantified with a mechanistic model coupling axis organogenesis and biomass allocation.

TABLE 9. *Observed and simulated values ('GreenLab-Retroaction' and 'Water-GreenLab' models) of the number of phytomers on the primary and secondary axes at 799 °Cd*

	Primary axis			Secondary axis		
Mean FTSW values	Mean observed value	Simulated value with 'GreenLab-Retroaction'	Simulated value with 'Water-GreenLab'	Mean observed value	Simulated value with 'GreenLab -Retroaction'	Simulated value with 'Water-GreenLab'
0·89	37·8[a]	36	36	278[a]	241	239
0·47	35·4[a]	36	34	196[b]	235	188
0·09	23·3[b]	36	24	59[c]	119	44
RRMSE		28·2 %	5·2 %		32·0 %	18·4 %

The mean observed values were those published in Lebon *et al.* (2006).
* The mean FTSW values were those observed from 350 °Cd to the end of the experiment.
For the simulation results with GreenLab-Retroaction model, values were calculated with 50 repetitions of the simulation procedure.

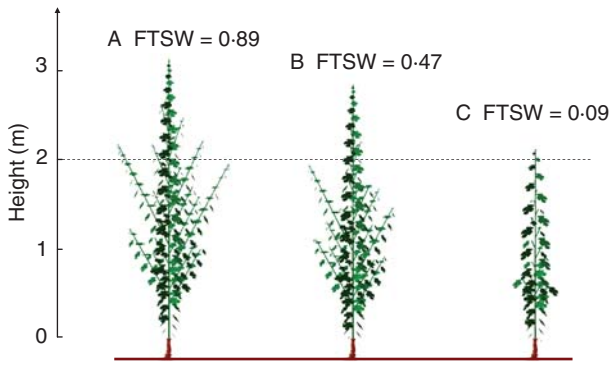

FIG. 5. Visualization of simulation results ('Water-GreenLab' model), 799 °Cd after budburst, with input parameters corresponding to the microclimate conditions used in expt 6. Before 350 °Cd, mean FTSW was 1, and after 350 °Cd, mean FTSW was 0·89 (A), 0·47 (B) or 0·09 (C). No data for internode length in well-watered conditions were available. The internode lengths were estimated from the allometric relationships estimated in well-watered conditions.

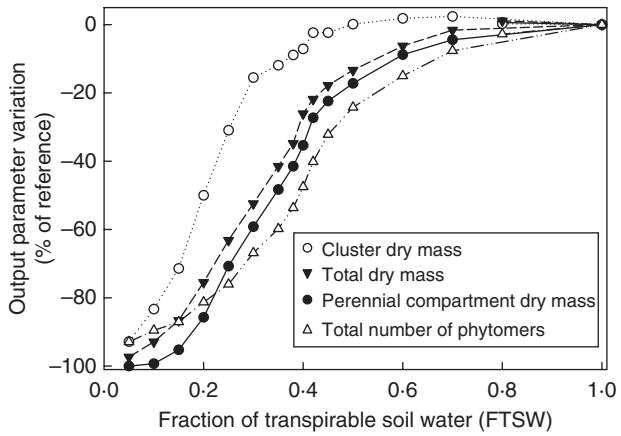

FIG. 6. Analysis of the sensitivity of the various outputs of the 'Water-GreenLab' model to fraction of transpirable soil water (FTSW) variations. The outputs values were normalized according to the values obtained for an FTSW of 1. Output values were calculated 1200 °Cd after budburst, with PPFD = 50 mol m^{-2} d^{-1}.

In previous studies using models based on the consideration of plant development as the result of source–sink relationships, some efforts were made to model plant development in conditions of fluctuating solar radiation (Dong *et al.*, 2008), but these models did not include feedback effects between plant functioning and organogenesis. In these previous studies, plant organogenesis was considered to be driven by temperature alone. Other models have included some relationships between trophic competition and plant organogenesis, but many of these studies remained theoretical (Cournède *et al.*, 2008; Mathieu *et al.*, 2009), or did not consider a fluctuating environment (Letort *et al.*, 2008). They focused on plants with lower levels of plasticity in organogenesis than the grapevine (e.g. rice; Luquet *et al.*, 2006) and they did not include water deficit effects. Previous versions of GreenLab (Kang *et al.*, 2008) also included stochastic relationships to take into account the variations observed in organogenesis and organ development. In this sudy a statistical approach was used to reproduce the observed quantitative relationships between plant development and their environment.

A heuristic approach to evaluate the determinants of axis organogenesis

By modelling the interactions between plant functioning (photosynthesis and trophic competition), plant development (rate of phytomer appearance and duration of axis development), plant anatomy (modular and branching structure) and microclimate (soil water deficit, photosynthetically active radiation and temperature) this study has increased our understanding about the construction of a complex phenotype. This heuristic approach focused principally on the behaviour of a population of meristems and revealed the role of various determinants of plant development in controlling meristem functioning.

The maximal rate of phytomer production according to temperature for each axis corresponds to the rate of phytomer appearence on the primary axis. This rate is equal to 0·044 phytomer per degree-days in 'well-watered' conditions (Lebon *et al.*, 2004) and it appears to be characteristic of a given genotype, or even of a species (Turc and Lecoeur, 1997). The inability of the other axes to exceed this maximal potential rate reflects the priority accorded to the primary apex in terms of biomass allocation. The differences in the rates of development of the P0 and P1–P2 secondary axes probably result from the overall effects of hormone signals in the hierarchical system (Shimizu-Sato and Mori,

2001). The balance of hormones in the axillary buds is probably determined by their initial growth rate at the start of axis development (Novoplansky, 1996). The short interval between the budburst dates of the different secondary axes within each module (Louarn *et al.*, 2007) probably confers an advantage on the P0 secondary axis in terms of sink strength and hormonal balance.

In the situation of lack of assimilate, the axillary meristems generate phytomers much more slowly. The functioning of the meristem is thus adjusted according to resource availability. This ability of the meristem to modulate its rate of development according to the carbon status of the plant has been confirmed by a number of experimental results. These studies demonstrated the control of genes involved in meristem activity by sugar signalling (Gibson, 2005; Ji *et al.*, 2005). This feedback control has been reported in a number of perennial plants (Wardlaw, 1990), and may constitute a specific adaptation of perennial plants. This specific adaption enables the perennial plants to avoid large decreases in reserve biomass (Dingkhun *et al.*, 2007; Silpi *et al.*, 2007). This hypothetical importance of the reserve sink may account for the lack of correlation between meristem functionning and carbon status in many annual plants displaying either determinate or indeterminate patterns of development [e.g. Turc and Lecoeur (1997) on pea; Granier and Tardieu (1999) on sunflower].

In the presence of a soil water deficit, the control of meristem activity by assimilate availability cannot account for the observed decrease in axis organogenesis. This finding is consistent with those of studies performed in conditions of moderate soil water deficit. In these studies an accumulation of soluble sugar in the plant in the soil water deficit condition was observed if the number of sinks is reduced before any decrease in photosynthesis activity (Tardieu *et al.*, 1999). This lack of connection between axis organogenesis and carbon status may be more marked in plants displaying an indeterminate pattern of development and truly anisohydric behaviour (Schultz, 2003). The early decrease in axis organogenesis is probably triggered by a hormonal signal originating in the roots (Sobeih *et al.*, 2004). ABA transport from the roots may modify the CK : ABA ratio, potentially increasing apical dominance (Stoll *et al.*, 2000).

The 'Water-GreenLab' model requires further validation with experimental data collected on plants grown in a microclimate in which both PPFD and FTSW are varied. However, this first validation of the 'Water-GreenLab' model and the demonstrated ability of the model to reproduce patterns of behaviour observed in viticulture indicates that water constraints should be included in models based on biomass fluxes. In the present study, only one genotype was used, with one set of parameters that were time-consuming to estimate on independent sets of plants. Further work on this model is required to reduce the number of parameters, making it possible to simulate the development of a wide range of cultivars. Some of the parameter identification procedures underlying the success of GreenLab for estimating hidden parameters parameters (Digiplant Software; Cournède *et al.*, 2006) should be developed further.

The 'GreenLab-Retroaction' and 'Water-GreenLab' models were calibrated and validated on plants grown in pots with simple architecture. Further experiments and implementations would be necessary to extrapolate these models to vineyard conditions including older plants and more complex architectural managements. In these models the representation of the perennial compartment is relevant for young plants with a high level of priority according to the storing reserve (Keller *et al.*, 1995; Pallas *et al.*, 2010). To enlarge the domain of validity of these models, a possible approach would be to generalize the organ formalism describing primary and secondary growth as well as the contribution of the organs to the plant biomass balance. For the perennial compartment it would be necessary to estimate the variations in the sink strength according to plant carbon status. For the vegetative organs, it would be also necessary to take into account their ability to stock biomass.

In this study, a single shoot is allowed to develop per plant whereas in classical vineyard conditions many shoots are kept per plant. In previous studies (e.g. Lebon *et al.*, 2004; Louarn *et al.*, 2007) it was observed that the development of each shoot on grapevine with a low number of vegetative shoots is quite similar to the development of one single shoot on a plant. In this case the plant can be assimilated to a population of independant shoots. Nevertheless for training systems in which a large number of vegetative shoots are kept, the level of development of each axis tends to decrease compared with the development of an isolated shoot (Miller *et al.*, 1996), especially for minimal pruning systems since this training system results in a 4-fold increased number of growing shoots (Dowton and Grant, 1992). In this case a hierarchy between each shoot in terms of biomass partitioning occurs and this hierarchy seems to be dependant on the timing of each axis budburst, and on hormonal balance (e.g. Novoplansky, 1996). Thus it would be necessary to take into account a whole plant carbon balance between each shoot according to their relative sink strength.

ACKNOWLEDGEMENTS

We thank M. Kawamata, C. Pons, A. Dardou, J. Mineau, M. Ferrand, E. T. Sumer, D. Merabet, D. Rablat, A. Seguard and H. Mallié for technical assistance during experiments, and Drs P. De Reffye and V. Letort for fruitful discussions.

LITERATURE CITED

Belaygue C, Wery J, Cowan AA, Tardieu F. 1996. Contribution of leaf expansion, rate of leaf appearance, and stolon branching to growth of plant leaf area under water deficit in white clover. *Crop Science* **36**: 1240–1246.

Candolfi-Vasconcelos MC, Candolfi MP, Koblet W. 1994. Retranslocation of carbon reserves from the woody storage as a response to defoliation stress during the ripening period in *Vitis vinifera* L. *Planta* **192**: 567–573.

Carbonneau A, Deloire A, Jaillard B. 2007. *La vigne: physiologie, terroir, culture.* Paris, France: Dunod.

Castelan-Estrada M. 2001. *Répartition de la biomasse chez* Vitis vinifera *L.; rendement de conversion du rayonnement solaire global et coûts énergétiques.* PhD Thesis, Institut national agronomique de Paris Grignon.

Chenu K, Chapman SC, Hammer Gl, McLean G, Ben Haj Salah H, Tardieu F. 2008. Short-term response of leaf growth rate to water deficit scale up to whole-plant and crop levels: an integrated modelling approach in maize. *Plant, Cell & Environment* **31**: 378–391.

Coombe BG. 1976. The development of fleshy fruits. *Annual Reviews of Plant Physiology* **27**: 507–528.

Coombe BG. 1995. Adoption of a system for identifying grapevine growth stages. *Australian Journal of Grape and Wine Research* **1**: 100–110.

Cournède PH, Kang M, Mathieu A, *et al*. 2006. Structural factorization of plants to compute their functional and architectural growth. *Simulation* **82**: 427–438.

Cournède PH, Mathieu A, Houllier F, Barthélémy D, de Reffye P. 2008. Computing competition for light in the Greenlab model of plant growth: a contribution to the study of the effects of density on resource acquisition and architectural development. *Annals of Botany* **101**: 1207–1218.

Davies WJ, Zhang J. 1991. Root signals and the regulation of growth and development of plants in drying soil. *Annual Review of Plant Physiology and Plant Molecular Biology* **42**: 55–76.

Dingkuhn M, Luquet D, Quilot B, de Reffye P. 2005. Environmental and genetic control of morphogenesis in crops: towards models simulating phenotypic plasticity. *Australian Journal of Agricultural Research* **56**: 1–14.

Dingkuhn M, Luquet D, Clément-Vidal A, Tambour L, Kin HK, Song YH. 2007. Is plant growth driven by sink regulation? Implications for crop models, phenotyping approaches and ideotypes. In: Sprietz JH, Struick PC, van Laar HH. eds. *Scale and complexity in plant research: gene–plant–crop relations*. Dordrecht: Springer, 157–170.

Dong Q, Louarn G, Wang Y, Barczi JF, de Reffye P. 2008. Does the structure-function model GREENLAB deal with crop phenotypic induced by plant spacing? A case study on tomato. *Annals of Botany* **101**: 1195–1206.

Downton WJS, Grant WJR. 1992. Photosynthetic physiology of spur pruned and minimal pruned grapevines. *Australian Journal of Plant Physiology* **19**: 309–316.

Flexas J, Bota J, Escalona MJ, Sampol B, Medrano H. 2002. Effects of drought on photosynthesis in grapevines under field conditions: an evaluation of stomatal and mesophyll limitations. *Functional Plant Biology* **29**: 461–471.

Gibson SI. 2005. Control of plant development and gene expression by sugar signaling. *Current Opinion in Plant Biology* **8**: 93–102.

Granier C, Tardieu F. 1999. Water deficit and spatial pattern of leaf development: variability in responses can be simulated using a simple model of leaf development. *Plant Physiology* **119**: 609–620.

Guo Y, Ma Y, Zhigang Z, *et al*. 2006. Parameter optimization and field validation of the functional-structural model GREENLAB for maize. *Annals of Botany* **97**: 217–230.

Heuvelink E. 1995. Dry matter partitioning in a tomato plant: one common assimilate pool? *Journal of Experimental Botany* **46**: 1025–1033.

Hsiao TC. 1973. Plant responses to water stress. *Annual Review of Plant Physiology* **24**: 519–570.

Huglin P. 1986. *Biologie et écologie de la vigne*. Lausanne, Switzerland: Payot.

Jaquinet A, Simon JL. 1971. Contribution à l'étude de la croissance des rameaux de vigne. *Revue Suisse de Viticulture, d'Arboriculture et d'Horticulture* **3**: 131–135.

Ji X, Van den Ende W, Van Laere A, Cheng S, Bennet J. 2005. Structure, evolution and expression of the two invertase gene families in rice. *Journal of Molecular Evolution* **60**: 615–634.

Johnson IR, Thronley JHM. 1985. Temperature dependence of plant and crop processes. *Annals of Botany* **55**: 1–24.

Kang M, Cournede PH, de Reffye P, Auclair D, Hu B. 2008. Analytical study of a stochastic plant growth model: application to the GreenLab model. *Mathematics and Computers in Simulation* **78**: 57–75.

Keller M, Hess B, Schwager H, Schärer H, Koblet W. 1995. Carbon and nitrogen partitioning in *Vitis vinifera* L.: responses to nitrogen supply and limiting irradiance. *Vitis* **34**: 19–26.

Koblet W, Perret P. 1972. Wanderung von Assimilaten innerhalb der Rebe. *Wein-Wiss* **27**: 146–154.

Lebon E, Pellegrino A, Tardieu F, Lecoeur J. 2004. Shoot development in grapevine (*Vitis vinifera* L.) is affected by the modular branching pattern of the stem and intra-inter-shoot trophic competition. *Annals of Botany* **46**: 1093–1101.

Lebon E, Pellegrino A, Louarn G, Lecoeur J. 2006. Branch development controls leaf area dynamics in grapevine (*Vitis vinifera)* growing in drying soil. *Annals of Botany* **98**: 175–185.

Letort V. 2008. *Analyse multi-échelle des relations source-puits dans les modèles de croissance des plantes pour l'identification paramétrique. Cas du modèle GreenLab*. PhD Thesis, Ecole Centrale de Paris, France.

Letort V, Cournède PH, Mathieu A, de Reffye P, Constant T. 2008. Parametric identification of a functional-structural tree growth model and application to beech trees. *Functional Plant Biology* **35**: 951–968.

Louarn G, Guedon Y, Lecoeur J, Lebon E. 2007. Quantitative analysis of the phenotypic variability of shoot architecture in two grapevine cultivars (*Vitis vinifera* L.). *Annals of Botany* **99**: 425–437.

Luquet D, Dingkuhn M, Kim H, Tambour L, Clement-Vidal A. 2006. *EcoMeristem*, a model of morphogenesis and competition among sinks in rice. 1. Concept, validation and sensitivity analysis. *Functional Plant Biology* **33**: 309–323.

Ma Y, Wen M, Guo Y, Li B, Cournède PH, de Reffye P. 2008. Parameter optimization and field validation of the functional-structural model GreenLab for maize at different population densities. *Annals of Botany* **101**: 1185–1194.

Mäkela A. 1986. Partitioning coefficients in plant models with turn-over. *Annals of Botany* **57**: 291–297.

Mathieu A, Cournède PH, Letort V, Barthélémy D, de Reffye P. 2009. A dynamic model of plant growth with interactions between development and functional mechanisms to study plant structural plasticity related to trophic competition. *Annals of Botany* **103**: 1173–1186.

Meziane D, Shipley B. 1999. Interacting determinants of specific leaf area in 22 herbaceous species: effects of irradiance and nutrient availability. *Plant, Cell & Environment* **22**: 447–459.

Miller DP, Howell GS, Flore JA. 1996. Effect of shoot number on potted grapevines. I. Canopy development and morphology. *American Journal of Enology and Viticulture* **47**: 244–250.

Monteith JL. 1977. Climate and the efficiency of crop production in Britain. *Philosophical Transactions of the Royal Society of London* **281**: 277–294.

Novoplansky A. 1996. Hierarchy establishment among potentially similar buds. *Plant, Cell & Environment* **19**: 781–786.

Pallas B, Louarn G, Christophe A, Lebon E, Lecoeur J. 2008. Influence of intra-shoot trophic competition on shoot development of two grapevine cultivars (*Vitis vinifera* L.). *Physiologia Plantarum* **134**: 49–63.

Pallas B, Christophe A, Cournède PH, Lecoeur J. 2009. Using a mathematical model to evaluate the trophic and non-trophic determinants of axis development in grapevine. *Functional Plant Biology* **36**: 156–170.

Pallas B, Christophe A, Lecoeur J. 2010. Are the common assimilate pool and trophic relationships appropriate for dealing with the observed plasticity of grapevine development. *Annals of Botany* **105**: 233–247.

Rives M. 2000. Vigour, pruning, cropping in the grapevine (*Vitis vinifera* L.). I. A literature review. *Agronomie* **20**: 79–91.

Schultz HR. 1992. An empirical model for the simulation of leaf appearance and leaf development of primary shoots of several grapevine (*Vitis vinifera* L.) canopy systems. *Scientia Horticulturae* **52**: 179–200.

Schultz HR. 2003. Differences in hydraulic architecture account for near-isohydric and anisohydric behaviour of two field-grown *Vitis vinifera* L. cultivars during drought. *Plant, Cell & Environment* **26**: 1393–1405.

Shipley B, Meziane D. 2002. The balanced-growth hypothesis and the allometry of leaf and root biomass allocation. *Functional Ecology* **16**: 326–331.

Shimizu-Sato S, Mori H. 2001. Control of outgrowth and dormancy in axillary buds. *Plant Physiology* **127**: 1405–1413.

Shinozaki K, Yoda K, Hozumi K, Kira T. 1964. A quantitative analysis of plant form: the Pipe model theory. I. Basic analyses. *Japanese Journal of Ecology* **14**: 97–105.

Silpi U, Lacointe A, Kasempsap P, *et al*. 2007. Carbohydrate reserve as a competitive sink: evidence from tapping rubber trees. *Tree Physiology* **27**: 881–889.

Sinclair TR, Ludlow MM. 1986. Influence of soil water supply on the plant water balance of four tropical grain legumes. *Australian Journal of Plant Physiology* **13**: 329–341.

Sobeih W, Dodd IC, Bacon MA, Grierson D, Davies WJ. 2004. Long-distance signals regulating stomatal conductance and leaf growth in tomato (*Lycopersicon esculentum*) plants subjected to partial root-zone drying. *Journal of Experimental Botany* **55**: 2353–2363.

Stevens RM, Pech JM, Gibberd MR, *et al*. 2008. Effect of reduced irrigation on growth, yield, ripening rates and water relations of Chardonnay vines grafted onto five rootstocks. *Australian Journal of Grape and Wine Research* **14**: 177–190.

Stoll M, Loveys B, Dry P. 2000. Hormonal changes induced by partial root-zone drying of irrigated grapevine. *Journal of Experimental Botany* **49**: 419–432.

Tardieu F, Granier C, Muller B. 1999. Modelling leaf expansion in a fluctuating environment: should we use an equation describing carbon budget, tissue expansion or cell division? *New Phytologist* **143**: 33–43.

Turc O, Lecoeur J. 1997. Leaf primordium initiation and expanded leaf production are co-ordinated responses to air temperature in pea (*Pisum sativum* L.). *Annals of Botany* **80**: 265–273.

Vose JM, Sullivan NH, Clinton BD, Bolstad PV. 1995. Vertical leaf area distribution, light transmittance, and application of the Beer-Lambert law in four mature hardwood stands in the southern Appalachians. *Canadian Journal of Forest Research* **25**: 1036–1043.

Wardlaw I. 1990. The control of carbon partitioning in plants. *New Phytologist* **116**: 341–381.

Yan H, Kang M, de Reffye P, Dingkuhn M. 2004. A dynamic, architectural plant model simulating resource-dependant growth. *Annals of Botany* **93**: 591–602.

Yin X, Goudriaan J, Lantinga EA, Vos J, Spiertz HJ. 2003. A flexible sigmoid function of determinate growth. *Annals of Botany* **91**: 361–371.

Zapata C, Deléens E, Chaillou S, Magné C. 2004. Mobilisation and distribution of starch and total N in two grapevine cultivars differing in their susceptibility to shedding. *Functional Plant Biology* **31**: 1127–1135.